



On the Normal-Incidence Reflection Coefficient in Porous Media

José M. Carcione^{1,2} · Davide Gei² · Boris Gurevich³ · Jing Ba¹

Received: 5 January 2021 / Accepted: 17 April 2021
© The Author(s), under exclusive licence to Springer Nature B.V. 2021

Abstract

We compare the exact normal-incidence PP reflection coefficient [Geertsma–Smit expression] to approximations reported by several authors, based on open-pore boundary conditions at a plane interface between two porous media. The approximations correspond to low frequencies. Two of them are derived from the low-frequency Biot theory below the Biot characteristic frequency, but the results show significant differences much below the Biot frequency. Then, we extend the Geertsma–Smit equations by including the high-frequency viscodynamic operator (i.e., the full-frequency range Biot theory), showing that there are additional substantial differences at the high-frequency range. Use of this latter expression is required to honor the physics in the whole frequency range. We further generalize the Geertsma–Smit equations to the case of general boundary conditions other than the open-pore interface. At the seismic band, it is shown that the lossless (elastic) expression based on the Gassmann P-wave impedance is the reflection coefficient to use for practical applications. It is inferred that interpretations based on the frequency dependency of these approximations can be misleading, since this dependency does not provide a suitable description of the physics.

Keywords Reflection coefficient · Porous media · Biot theory · Normal incidence

Article Highlights

- We compare the exact normal-incidence PP reflection coefficient in porous media to approximations reported by several authors, based on open-pore boundary conditions
- Two of the coefficients are intended to be approximations below the Biot characteristic frequency, but the results show significant differences with the exact one much below this frequency

✉ Jing Ba
jba@hhu.edu.cn

¹ School of Earth Sciences and Engineering, Hohai University, Nanjing 211100, Jiangsu, China

² Istituto Nazionale di Oceanografia e di Geofisica Sperimentale (OGS), Borgo Grotta Gigante 42c, 34010 Sgonico, Trieste, Italy

³ Department of Exploration Geophysics, Curtin University, GPO Box U1987, Perth, WA 6845, Australia

- We extend the exact coefficient by including the high-frequency viscodynamic operator and general boundary conditions other than the open-pore interface

1 Introduction

The acoustics of porous media finds applications in several fields, such as hydrocarbon exploration (Bourbie et al. 1987), polymer physics (Johnson 1982), the food industry (Carcione et al. 2007) and general acoustics (Allard 1993). The theory of poroelasticity gives a suitable description of the physics of wave propagation. In particular, Biot's theory shows that, in a poroelastic medium, there may exist two compressional waves: the so-called fast and slow waves, as well as a shear wave (Biot 1956a, b, 1962; Bourbie et al. 1987). At frequencies above Biot's characteristic frequency, the slow wave is propagatory with a velocity controlled largely by the sound velocity in a free fluid (Johnson and Plona 1982). On the other hand, at frequencies below Biot's characteristic frequency, the slow wave is diffusive (with diffusivity controlled by the matrix permeability and pore fluid viscosity) and hence attenuates right near the source (e.g., Carcione and Quiroga-Goode 1995). Thus, the only wave observed in seismic data at low frequencies is the fast compressional wave, which has very small dispersion and attenuation, and its velocity is not effected by viscous friction between solid and fluid (and hence is independent of permeability) (e.g., Biot 1956a; Johnson 1982; Gurevich 1994). Yet viscous coupling (controlled by the matrix permeability and pore fluid viscosity) may play a role near interfaces between different porous layers, due to mode conversion and energy re-partition between the fast and slow waves at interfaces (e.g., Deresiewicz and Rice 1964; Dutta and Odé 1983). Thus, it has been suggested that reflection coefficients between adjacent porous layers may be affected by viscosity and permeability, and thus can be used to estimate permeability and/or fluid viscosity from seismic reflection data (Silin et al. 2006; Silin and Goloshubin 2010; Xu et al. 2011; Li and Rao 2020). Therefore, it is important to explore the viscosity–permeability dependence of reflection coefficients.

In this work, we investigate the normal-incidence reflection coefficient at an interface between two dissimilar porous media saturated with viscous fluids. Two approximations, based on Biot theory, are reported in the literature, namely by Bourbie et al. (1987) and by Gurevich et al. (2004), while the exact solution for an open-pore interface has been published by Geertsma and Smit (1961) in the framework of the low-frequency theory (Biot 1956a). A third approximation has been reported by Silin and Goloshubin (2010) and used to estimate permeability (Goloshubin et al. 2008) and fluid type (Xu et al. 2011; Li and Rao 2020) from seismic data. Zhou et al. (2020) derive an expression for a non-viscous fluid and claim to be the first to derive it, although the reflection coefficient in this case can easily be obtained by setting to zero the fluid viscosity in the Geertsma–Smit equations.

All the existing analyses are inconclusive, because they are based on approximations, whose exact range of validity is unknown. In this work, we investigate the normal-incidence reflection coefficient at an interface between two dissimilar porous media saturated with viscous fluids using exact expressions for reflections at interfaces. We compare expressions in the more significant case of a viscous fluid and generalize the Geertsma–Smit equations using the full frequency range viscodynamic operator and general boundary conditions (Quiroga-Goode and Carcione 1997). The latter can be classified into open, mixed and closed (Deresiewicz and Skalak 1963; Rasolofosaon 1988; Gurevich and Schoenberg 1999). In the first case, the pores of both media are completely connected, while in the

third the pores are disconnected (sealed interface). In the mixed case, the pores are partially connected so that the boundary equations are parameterized by a surface impedance that quantifies the amount of flow across the interface.

2 Reflection Coefficient

2.1 Review of the Approximations

The reported approximations of the normal-incidence reflection coefficient at a plane interface separating two porous media are given in [Appendix A](#), denoting the properties of the incidence medium 1 and transmission medium 2 with the subindices $j = 1$ and 2, respectively.

Bourbie et al. (1987) report the scattering coefficients for an open interface taken from two papers (Geertsma and Smit 1961; Deresiewicz and Rice 1964). If we define the Biot characteristic frequency

$$\omega_c = \frac{\phi\eta}{\kappa\rho_f}, \tag{1}$$

where ρ_f is the fluid density, ϕ is the rock porosity, κ is the permeability and η is the fluid viscosity. The equations correspond, apparently, to an expansion to the nearest second order in ω/ω_c , since it is not clear what the type of approximation is in the book on the basis of the equations of the two preceding papers.

Gurevich et al. (2004) obtained the scattering coefficients from a plane interface under the low-frequency approximation, below the Biot characteristic frequency, by which the relative displacement of the fluid with respect to the solid within the fast wave is negligible. The Fourier convention is $\exp(-i\omega t)$. This allows them to simplify the wavenumbers of the fast and slow waves (their Eqs. 10 and 11).

Silin and Goloshubin (2010) express the reflection coefficient in terms of a frequency-dependent dimensionless parameter, which is the product of the reservoir fluid mobility (i.e., inverse viscosity), fluid density and frequency of the signal. They state that the results are obtained through a low-frequency asymptotic analysis of Biot model of poroelasticity. However, their zero-frequency reflection coefficient is not Gassmann consistent.

2.2 Exact expression

In this section, we consider the exact scattering coefficients obtained by Quiroga-Goode and Carcione (1997), who generalized the equations of Geertsma and Smit (1961) to mixed and closed boundary conditions. In this case, we denote the properties of media 1 and 2 with unprimed and prime superscripts to ease the identification of the equations in the last paper. Denoting u , w , σ and p the solid displacement, the fluid displacement relative to the solid, the solid stress and the fluid pressure, respectively, the general boundary conditions at the interface are

$$u = u', \quad w = w', \quad \sigma = \sigma', \quad p = p' + k\dot{w}, \quad (\text{or } u_1 = u_2, \quad w_1 = w_2, \quad \sigma_1 = \sigma_2, \quad p_1 = p_2 + k\dot{w}), \tag{2}$$

where k is the coefficient of resistance, also called surface flow impedance and a dot above a variable indicates time differentiation (Carcione 2014; Eq. 7.404). The unit of k is Pa · s/m.

The meaning of k is explained in Deresiewicz and Skalak (1963) as partially communicating pores between the two media, but can also be related to a thin layer at the interface characterized by k . An example is a mud cake much thinner than the wavelength in a borehole (Rosenbaum 1974).

Equations (2) models three types of boundary conditions:

1. $k = 0$ (open interface, pores communicate).
2. $k = \infty$ (sealed interface, pores do not communicate).
3. $0 < k < \infty$ (partially open interface).

As above, we consider an incident fast P wave. Then, in Eqs. (57)–(58) of Geertsma and Smit (1961) we have $A_{1i} = 1$, $A_{1r} = R_1 = R$, $A_{2i} = 0$, $A_{2r} = R_2$, $A'_1 = T_1 = T$, $A'_2 = T_2$, where the subscripts “i” and “r” denote incident and reflected, respectively, R is the reflection coefficient of the fast P wave, and R_2 , T and T_2 correspond to the converted slow P wave reflection, fast P wave transmission and slow P wave transmission, respectively. Using their notation, the exact coefficients can be obtained from the following matrix equation:

$$\begin{bmatrix} 1 & 1 & -1 & -1 \\ m_1 & m_2 & -m'_1 & -m'_2 \\ D_1 & D_2 & D'_1 & D'_2 \\ F_1 & F_2 & (F'_1 - \omega km'_1) & (F'_2 - \omega km'_2) \end{bmatrix} \begin{bmatrix} R \\ R_2 \\ T \\ T_2 \end{bmatrix} = \begin{bmatrix} -1 \\ -m_1 \\ D_1 \\ F_1 \end{bmatrix}, \tag{3}$$

where

$$D_i = l_i(H - m_iK), \quad F_i = l_i(K - m_iL), \quad i = 1, 2, \tag{4}$$

and respective primed versions, where the subscripts 1 and 2 refer to the fast and slow P waves, respectively. In our notation, $L = M$, $H = E_G$ and $K = \alpha M$ [see Eqs. (19) and (20) and Appendix A for the definitions of the various quantities]. The wavenumbers l_i are solutions of the dispersion equation (20) in Geertsma and Smit (1961). With our notation:

$$\left| \begin{array}{c} z - 1 \\ \left(\frac{\rho_f}{\rho} - \frac{\alpha Mz}{E_G} \right) \end{array} \right| \begin{pmatrix} \left(\frac{\rho_f}{\rho} - \frac{\alpha Mz}{E_G} \right) \\ \left(\frac{Mz}{E_G} - \frac{Y}{i\omega\rho} \right) \end{pmatrix} = 0, \quad z_i = \frac{E_G l_i^2}{\rho\omega^2}, \quad i = 1, 2, \tag{5}$$

where

$$Y = \frac{i\omega\rho_f\mathcal{T}}{\phi} + \frac{\eta}{\kappa} \tag{6}$$

is the low-frequency viscodynamic operator (Biot 1956a; Carcione 2014, Eq. 7.272), where ρ_f is the fluid density, ϕ is the porosity, \mathcal{T} the pore-space tortuosity, η is fluid viscosity and κ is the permeability. Note that this property does not appear in the approximate theories. Furthermore,

$$m_i = \frac{(z_i - 1)E_G}{z_i \alpha M - (\rho_f / \rho) E_G} \tag{7}$$

and corresponding primed version, where ρ is the bulk density [see Eq. (21)].

Equation (3) is similar to Eq. (28) in Quiroga-Goode and Carcione (1997), which is a generalization of the Geertsma–Smit expression by including the interface impedance. In this work, the Fourier convention is $\exp(+i\omega t)$ and the wavenumbers obtained from Eq. (5) have opposite signs to the approximate ones [Eq. (22)]. Therefore, a comparison between the Geertsma and Smit reflection coefficient and that of Gurevich et al. requires to change the sign of ω in one of the expressions. Then, we change the sign of ω in Eq. (24). The convention in Bourbie et al. (1987) and Silin and Goloshubin (2010) is that of Geertsma and Smit (1961).

2.3 The High-Frequency Viscodynamic Operator

We further generalized Geertsma and Smit equations to include the high-frequency viscodynamic operator. Note that term “high-frequency” was introduced by Biot (1956b), but the operator holds for all frequencies. A boundary layer develops in the pore walls as frequency increases, where the microvelocities are out of phase. This layer, which becomes very thin at high frequencies, confines the viscous forces and the microvelocity. The friction force exhibits a complex and frequency-dependent quantity termed viscodynamic operator, which can be interpreted as complex viscosity, tortuosity or permeability [e.g., Carcione 2014, Eq. (7.276)]. To investigate the frequency range of validity of the viscodynamic operator (6), we consider a simple pore geometry, i.e., fluid flow in a plane slit of width h (flow between parallel walls). This problem has been solved by Biot (1956b), obtaining

$$Y_B = \frac{4\eta}{h^2} \left[\frac{q^2}{1 - (1/q)\tanh(q)} \right]. \tag{8}$$

where

$$q = \frac{h}{2} \sqrt{\frac{i\omega\rho_f}{\eta}} \tag{9}$$

(Carcione 2014). At low frequencies ($q \rightarrow 0$), we obtain $Y = 12\eta/h^2$. Comparing this equation with (6), we have $\kappa = h^2/12$. Let us assume that the pore space is made of many identical parallel plane slits. Then, the permeability depends not only on the slit width but also on the number of slits per unit length. The extension of the preceding equation to this case yields $\kappa = \phi h^2/12$. Then

$$h = 2\sqrt{\frac{3\kappa}{\phi}}. \tag{10}$$

Replacing this equation into (8) and dividing by ϕ to match (6) at low frequencies, we obtain

$$Y = \frac{i\omega\rho_f\phi^{-1}}{1 - (1/q)\tanh(q)}, \quad q = \sqrt{\frac{3i\omega\rho_f\kappa}{\phi\eta}}. \tag{11}$$

Use of the viscodynamic operator corresponding to circular tubes yields similar results, since it has the same limits as a function of frequency and crossover frequencies of the slit one (Biot 1956b; Eq. 3.15). Moreover, Carcione (2014, Fig. 7.8) showed that the difference between the slit operator and the more general heuristic operator proposed by Johnson et al. (1987) is small. In fact, it can be shown that the results are similar.

3 Examples

Let us consider the properties shown in Table 1, where the fluids in the incidence and transmission media are brine and gas, respectively, and the case of open boundary conditions. Porosity and permeability are related by the Kozeny–Carman relation (Mavko et al. 2009, p. 403)

$$\kappa = \frac{4B\phi^3 R^2}{(1-\phi)^2}, \quad (12)$$

where R is the grain radius and $B = 0.003$, and we assume $R = 80 \mu\text{m}$. We use the Krief model (Krief et al. 1990) and assume a Poisson medium to obtain the dry-rock moduli as

$$K_m = K_s(1-\phi)^{3/(1-\phi)} \quad \text{and} \quad \mu = \frac{3}{5}K_m. \quad (13)$$

Tortuosity is given by

$$\mathcal{T} = 1 - \frac{1}{2} \left(1 - \frac{1}{\phi} \right). \quad (14)$$

Equations (12)–(14) can be found in Mavko et al. (2009).

Figure 1 shows the exact phase velocities obtained from the wavenumbers, solutions of Eq. (5) as $c = 1/\text{Re}(1/\nu)$, where $\nu = \omega/l$ is the complex velocity (e.g., Carcione 2014). The comparison between the exact and approximated wavenumbers of Gurevich et al. (1994) [Eq. (22)] is displayed in Fig. 2 (incidence medium). Although the theory is valid up to the characteristic frequency (vertical line), some discrepancies at sonic frequencies are evident, but the approximation is valid at seismic frequencies.

Table 1 Material properties

Property	Incidence medium	Transmission medium
K_s (GPa)	39	39
K_f (GPa)	2.25	0.012
ρ_s (kg/m ³)	2650	2650
ρ_f (kg/m ³)	1040	80
ϕ	0.2	0.3
η (Pa · s)	0.001	0.0001
K_m (GPa)	16.9	8.45
μ (GPa)	10.13	5.07
κ (darcy)	0.96	4.23
\mathcal{T}	3	2.16

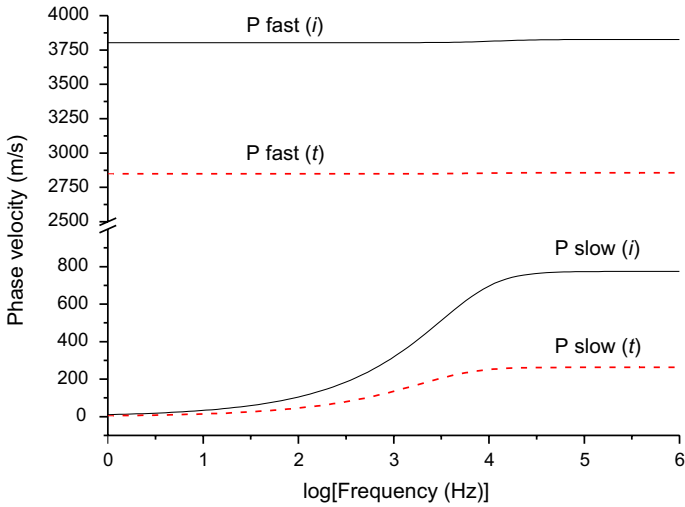


Fig. 1 Exact phase velocities of the incidence (black-solid curves) and transmission media (red-dashed curves). Phase velocities are obtained as $\omega/\text{Re}(l_j)$, $j = 1, 2$, where 1 and 2 denote the fast and slow waves, respectively (e.g., Carcione 2014)

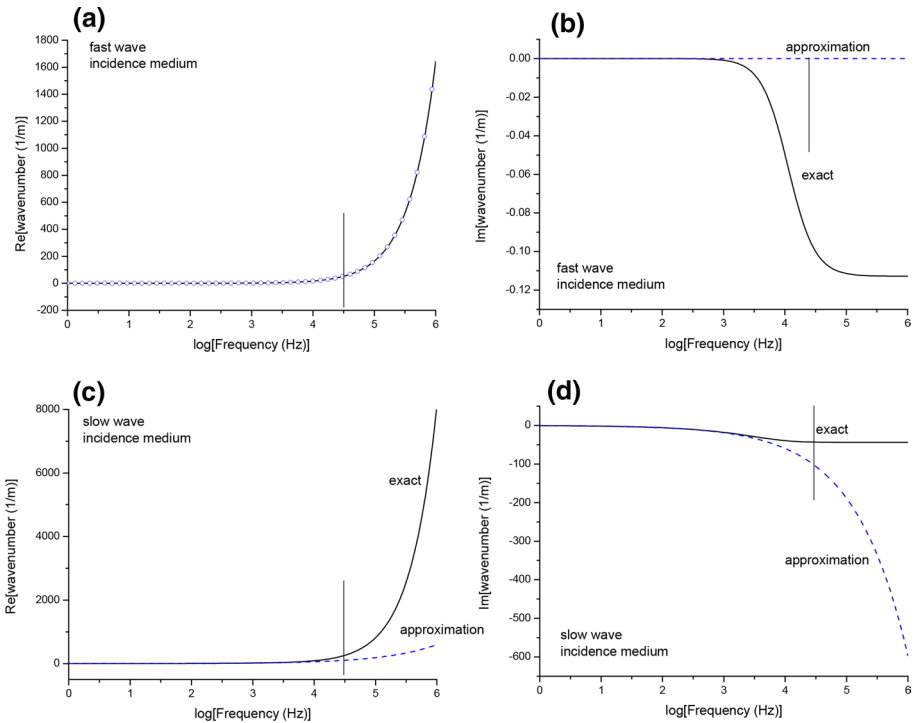


Fig. 2 Exact (black solid line) and approximated wavenumbers of Gurevich et al. (1994) (blue dots and dashed lines), corresponding to the incidence medium. The vertical line indicates the location of the characteristic frequency. The exact wavenumbers, l_j , are solutions of the dispersion Eq. (5) and those of Gurevich et al. (1994) are given by Eq. (22)

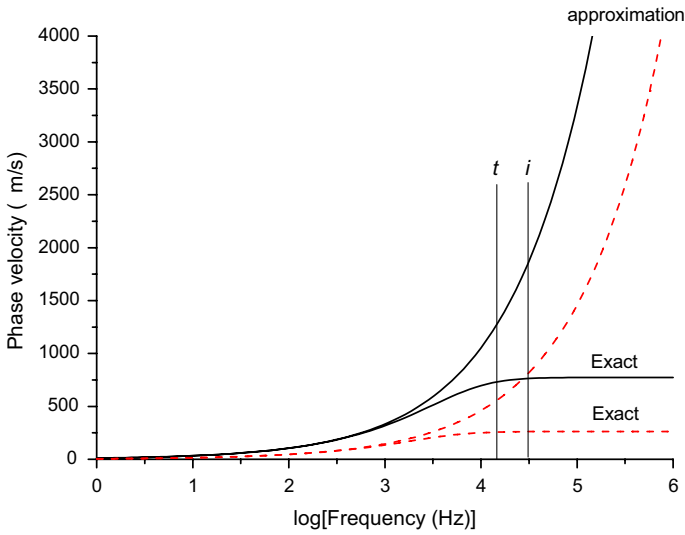


Fig. 3 Exact and approximated (Gurevich et al. 1994) phase velocities of the slow P wave in the incidence (black-solid curves) and transmission media (red-dashed curves). The vertical lines indicate the Biot characteristic frequencies of the incidence (*i*) and transmission (*t*) media. Phase velocities are obtained as $\omega/\text{Re}(l_j)$, $j = 1, 2$, where 1 and 2 denote the fast and slow waves, respectively (e.g., Carcione 2014)

Since the approximations (22) do not affect the fast P wave significantly, Fig. 3 compares the exact and approximate slow P wave velocities, where the vertical lines indicate the Biot characteristic frequencies of the incidence (*i*) and transmission (*t*) media. As can be seen, these approximations are valid below those reference frequencies.

Figure 4 shows the absolute value and phase of the reflection coefficients. The two curves denoted by 1 and 2 correspond to Eq. (26) computed with ϵ_1 and ϵ_2 , respectively. We can see that the approximate reflection coefficients substantially depart from the exact one above 1 KHz, while the Silin-Goloshubin coefficient is not Gassmann consistent at zero frequency. At 1 MHz and the entire band, we have the frequency-independent reflection coefficient

$$R_0 = \frac{Z_1 - Z_2}{Z_1 + Z_2}, \tag{15}$$

where here $Z = \sqrt{\rho E_G}$ is the Gassmann P-wave impedance and the presence of permeability, pore-space tortuosity and viscosity of the fluids have no effect. If we replace gas with water in medium 2, we obtain $R_0 = 0.15$ (against $R_0 = 0.25$ with gas) and on the basis of this value one could determine the presence of gas, but as we can see in Fig. 4, the effects of viscosity and permeability with frequency are negligible at the seismic band.

Let us consider a very low viscosity for both fluids, $\eta_1 = \eta_2 = 10^{-10}$ Pa · s, i.e., almost ideal or inviscid fluids. Since the frequency dependence in the low-frequency Biot theory is governed by the factor η/κ , this viscosity would correspond to an extremely high permeability of the order of 10^7 darcy for water. The absolute value of the reflection coefficient is shown in Fig. 5. The exact one (Geertsma–Smit) is in practice equal to R_0 and the approximations breakdown at seismological and seismic frequencies, because according to Eq. (1), the Biot characteristic frequency is very low. On the other hand, if we replace gas by oil

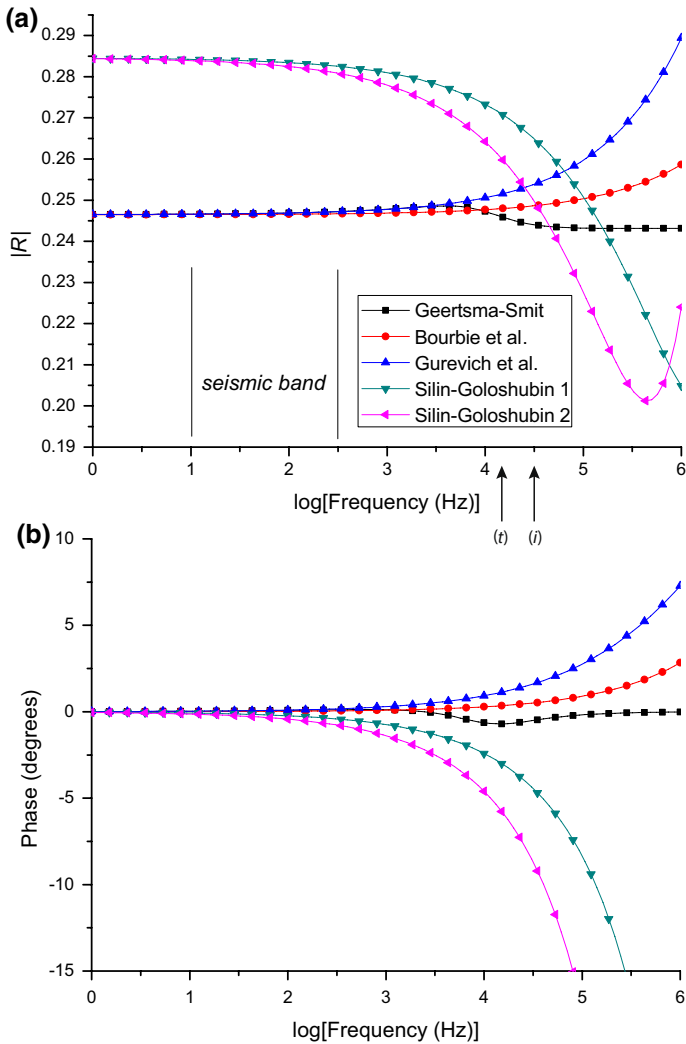


Fig. 4 Absolute value (a) and phase (b) of the PP reflection coefficient, where the Geertsma–Smit curve is the exact one (low-frequency Biot theory and open-pore conditions, but no approximations). The vertical arrows indicate the Biot characteristic frequencies of the incidence (i) and transmission (t) media

in Table 1, with a viscosity of $1 \text{ Pa} \cdot \text{s} = 1000 \text{ cP}$, it can be shown that the reflection coefficient in the frequency range shown in Fig. 5 and up to 1 kHz, is practically equal to its value at zero frequency, i.e., the Gassmann expression (15).

This is the same conclusion reached by Gurevich (1994): “...for an interface between two fluid-saturated porous media, the difference between poroelastic and elastic coefficients at seismic frequencies is only several percent, and the coefficients can be approximated by the elastic ones,” and by Gurevich et al. (1994), where the exact reflection coefficient of a thin layer compared to the effective Gassmann one has negligible

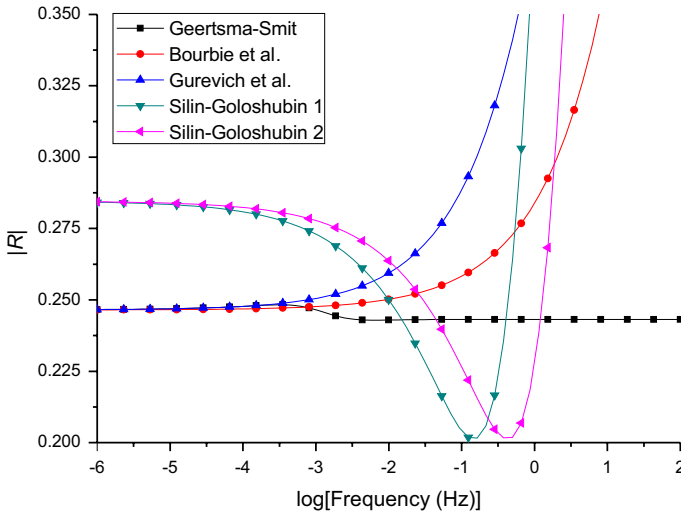


Fig. 5 Absolute value of the PP reflection coefficient for a very low viscosity of the fluids ($\eta_1 = \eta_2 = 10^{-10}$ Pa · s, i.e., almost ideal or inviscid fluids)

differences from a practical point of view. As shown by Carcione (1998, Fig 7), the effect of the slow wave can be seen when the medium has many heterogeneities. A single interface has no pronounced effect (Carcione 1998, Fig 8). The effect may become significant for a multi-layered porous medium, where the reflections may accumulate (White et al. 1975; Gurevich and Lopatnikov 1995; Carcione and Picotti 2006)

Let us now consider the properties in Table 1 and viscodynamic operator valid at all frequencies. Figure 6 shows the real (a) and imaginary parts (b) scaled by η/κ . Figure 6b compares the imaginary parts of the low-frequency and high-frequency operators, Eqs. (6) and (11), respectively. The differences can be noticed beyond 10 kHz, roughly the value of the Biot characteristic frequencies, which are 32 and 14 kHz for the incidence and transmission media, respectively.

Figure 7 shows the phase velocity (a) and dissipation factor (b) of the fast P wave, corresponding to the Geertsma–Smit theory, considering both the low- and high-frequency viscodynamic operators. The dissipation factor is computed with the quality factor $Q = \text{Re}(v^2)/\text{Im}(v^2)$ (e.g., Carcione 2014). We can see the relaxation peaks due to Biot global fluid flow mechanism, which are approximately centered at the characteristic frequency (1). The high-frequency Biot theory (dashed lines) has a better agreement with the reference frequency.

The absolute value (a) and phase (b) of the exact PP reflection coefficient, corresponding to the Geertsma–Smit equations are shown in Fig. 8. The solid-black and dashed-red lines refer to the low- and high-frequency viscodynamic operators, Eqs. (6) and (11), respectively. We observe that the inclusion of high-frequency effects highly affects the coefficient beyond the Biot characteristic frequencies.

Next, we analyze the effect of mixed and closed boundary conditions. We consider three values of the hydraulic permeability of the interface: $k = \infty$ (closed pores), 0 (open pores) and $10^7 \text{ s} \cdot \text{Pa/m}$ (mixed or partially open pores). The latter reciprocal value multiplied by viscosity, say water, corresponds to an effective of permeability of 100 darcy. The transition occurs at approximately $k = 10^8 \text{ s} \cdot \text{Pa/m}$. Above this value, the interface is practically

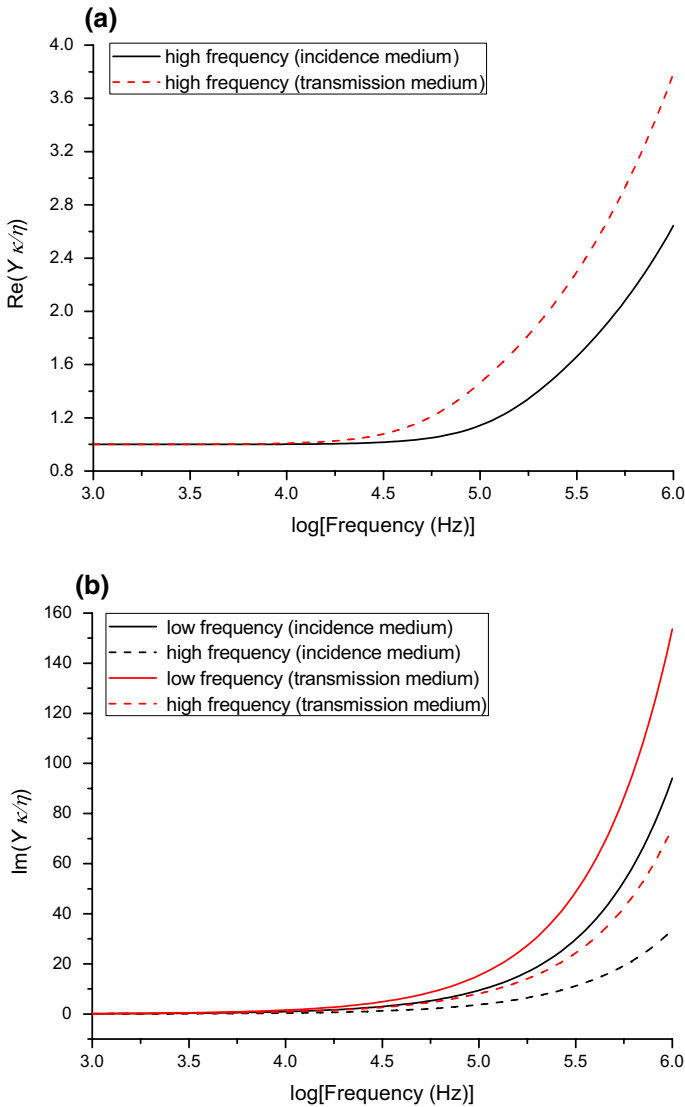


Fig. 6 Real (a) and imaginary parts (b) of the viscodynamic operator scaled by η/κ . In (a), the solid and dashed lines correspond to the high-frequency operator of the incidence and transmission media (the low-frequency one is constant and equal to the value at $\omega = 0$)

closed. The results (see Fig. 9) indicate that from a practical point view, the reflection coefficients do not differ. Differences between open- and sealed-pore conditions may be significant in the presence of air at room conditions, e.g., an interface separating water and air-filled porous media (Denneman et al. 2002), but this situation is not the case at depth in the Earth, since gas has the properties shown in Table 1 or behaves as a liquid at supercritical pressure–temperature conditions.

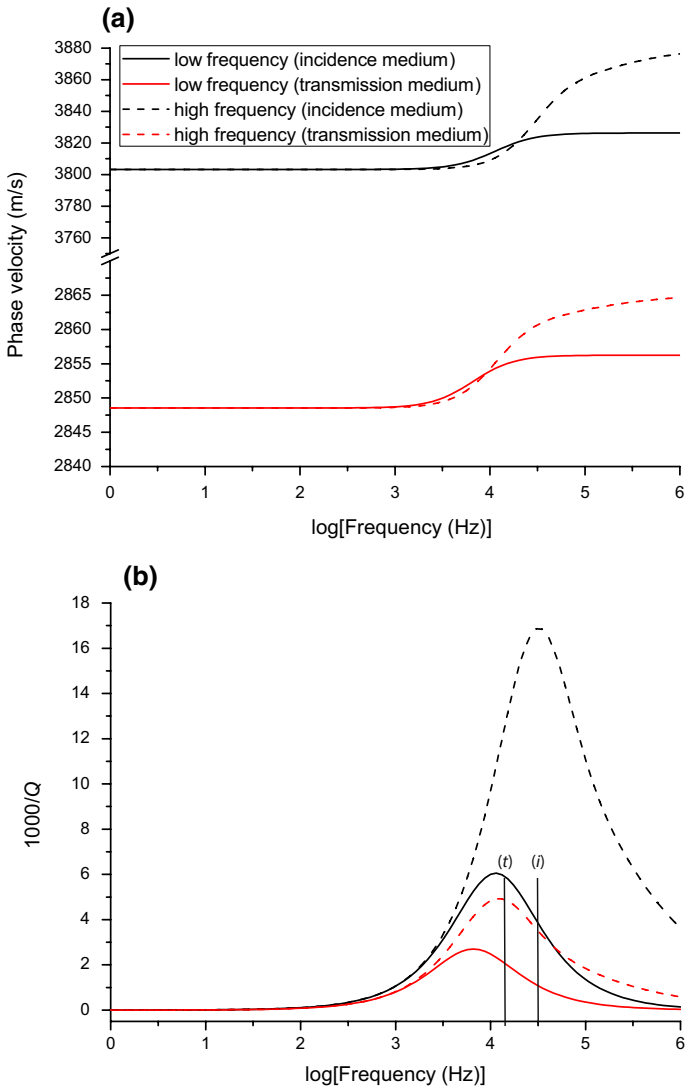


Fig. 7 Phase velocity (a) and dissipation factor (b) corresponding to the Geertsma–Smit theory. The vertical lines indicate the Biot characteristic frequencies of the incidence (*i*) and transmission (*t*) media. Phase velocities are obtained as $\omega/\text{Re}(l_j)$, $j = 1, 2$, where 1 and 2 denote the fast and slow waves, respectively, and $Q_j = -\text{Re}(l_j^2)/\text{Im}(l_j^2)$ (e.g., Carcione 2014)

To further analyze the effect of viscosity and permeability on the reflection coefficient at the seismic frequency band, we consider valid the low-frequency Biot theory, where viscosity and permeability are involved in a single quantity, i.e., $b = \eta/\kappa$. In the following example, we assume the matrix properties of Table 1 and brine in the upper and lower media, with $b_2 = b_1 = 10^9 \text{ kg}/(\text{m}^3\text{s})$ (a permeability of 1 darcy = 10^{-12} m^2), i.e., we do not use equation (12) to obtain the permeability. Now, we assume two other cases, where $b_2 = 10^4 b_1$ and $b_2 = 10^{-4} b_1$, corresponding to a lower medium whose

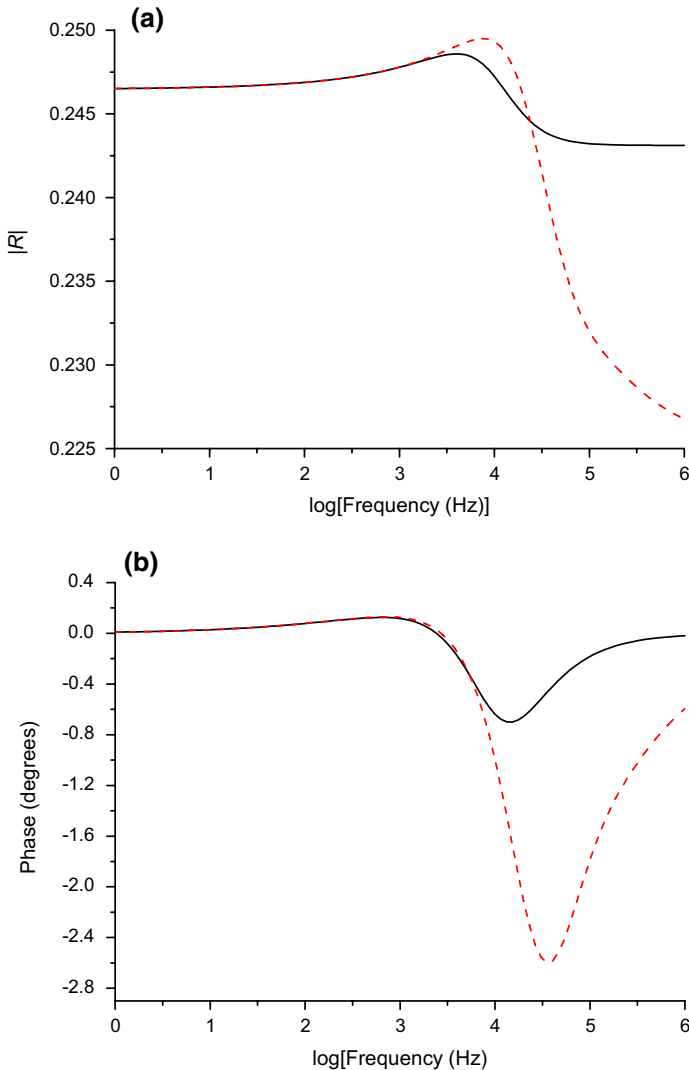


Fig. 8 Absolute value (a) and phase (b) of the exact PP reflection coefficient [see Eq. (3)], corresponding to the Geertsma–Smit equations, where the solid-black and dashed-red lines refer to the low- and high-frequency viscodynamic operators, Eqs. (6) and (11), respectively

permeability is reduced by a factor 10^4 or its viscosity is reduced by the same factor, respectively. These choices may correspond to shale or gas in the lower medium, respectively. Although, this assumption is unrealistic, since varying the permeability or the viscosity implies different porosity and dry-rock moduli in the first case, and different fluid bulk modulus and density in the second case, the purpose is solely to study the sensitivity to permeability and viscosity. Even in the most realistic case, it remains the uncertainty on the relations between permeability and porosity and dry-rock moduli, i.e., the parameters in the Kozeny–Carman and Krief equations. Figure 10 shows the

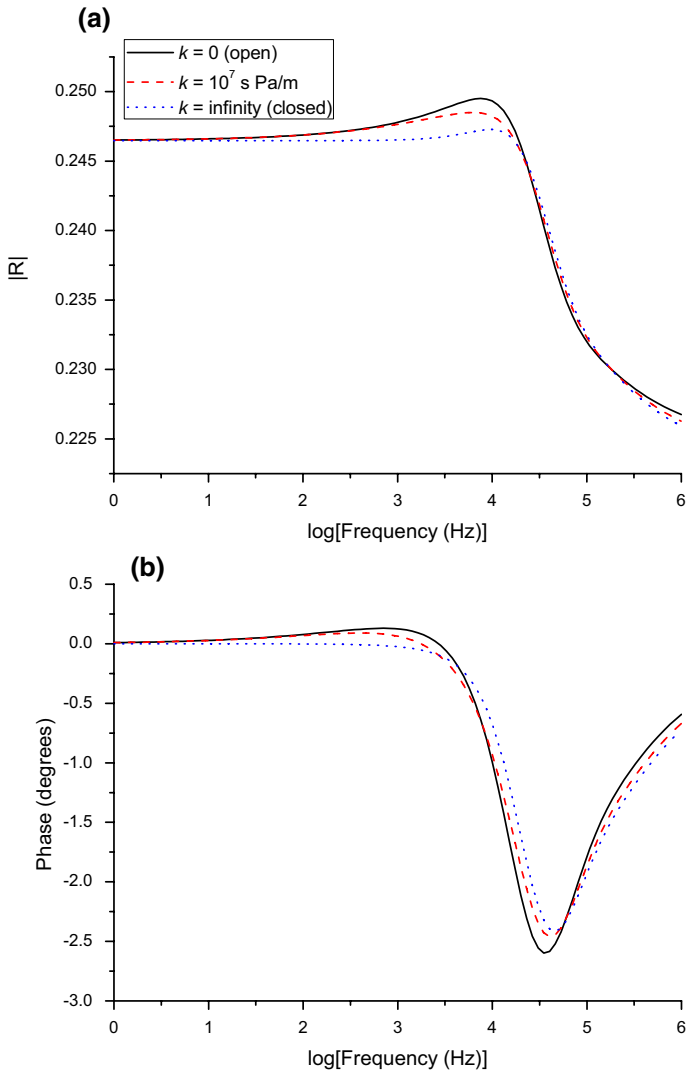


Fig. 9 Absolute value (a) and phase (b) of the exact PP reflection coefficient [see Eq. (3)], corresponding to the Geertsma–Smit equations for different boundary conditions at the interface. We have considered the high-frequency viscodynamic operator (11)

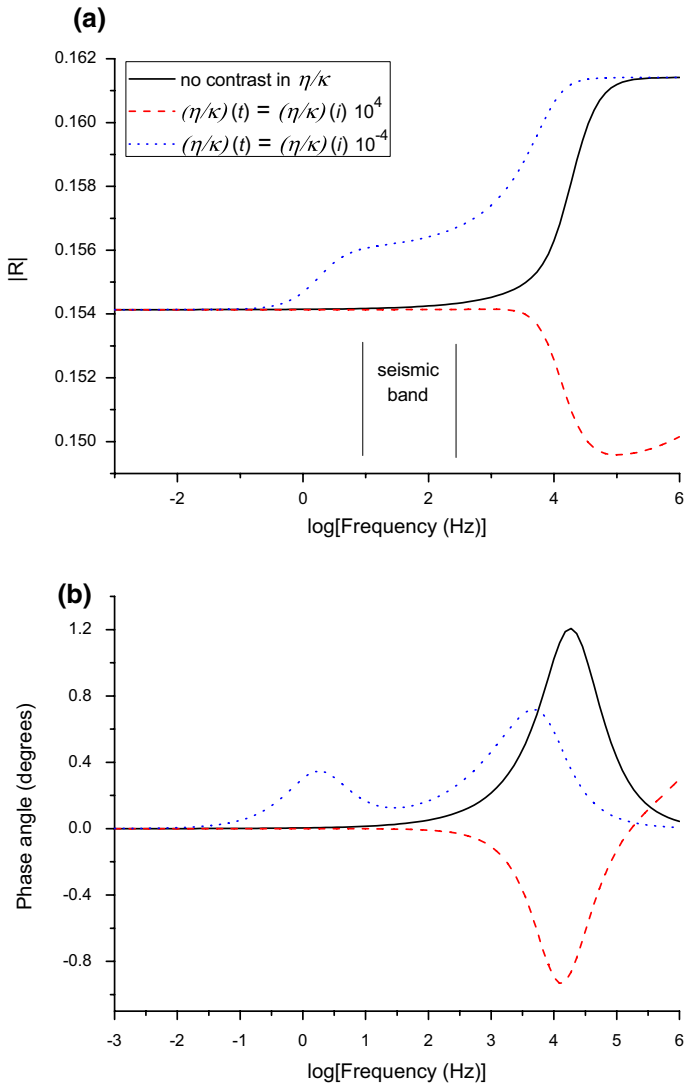


Fig. 10 Exact (Geertsma–Smit) absolute value **(a)** and phase **(b)** of the PP reflection coefficient as a function of frequency for low permeability (red dashed line) and low viscosity (blue dotted line) in the lower (transmission) medium. *(i)* and *(t)* indicate incidence (upper) and transmission (lower) media, respectively

exact (Geertsma–Smit) absolute value (a) and phase angle (b) of the PP reflection coefficient as a function of frequency for low permeability (red dashed line) and low viscosity (blue dotted line) in the lower (transmission) medium. It is clear that at the seismic band the changes in the reflection coefficients preclude any prediction based on these properties. Variations in amplitude of 0.02 and phase angle of 0.4° can hardly be detected in real data.

Our examples show very small variation of the reflection coefficient and phase angle within the seismic band. One may argue that the media can be described as patchy saturated, causing mesoscopic attenuation (Pride et al. 2003; Carcione 2014, Sections 7.13 and 7.14) and that in this case the corresponding reflection coefficient shows a higher sensitivity to viscosity and permeability. However, this is something that requires further research. Moreover, it remains the uncertainty of inverting for seismic Q from reflection data and on the size of the patches, and how to process the data to remove the effect of the overburden and reach the target at its real amplitude.

4 Conclusions

This work reviews and compares different reported expressions of the normal-incidence reflection coefficient in porous media, in order to establish their reliability, validity in different frequency bands and practical uses in seismic prospecting. It is clear from the example (and one suffices) that the effects of viscosity and permeability are too small to be detected in seismic data, even using the exact expression of the reflection coefficient. Including the viscodynamic operator greatly affects the reflection coefficient at high frequencies, beyond the Biot characteristic frequency of the order of tens of kHz. We have also considered the effects of the boundary condition and found that the difference between open- and closed-pore reflection coefficients is small. This review of the different approximations has as a main result that a misuse of them can lead to erroneous conclusions. Many cases can be set up to show this fact, but it is enough one example to reveal the limitations.

Appendix A: Approximations of the Normal-Incidence Reflection Coefficient

A.1 Bourbie et al. Equations

The normal-incidence PP reflection coefficient at an interface separating the incidence medium 1 and the transmission medium 2 reported by Bourbie et al. (1987) is

$$R = \frac{1 - Z}{1 + Z} \cdot (1 + \beta) \exp(i \tan^{-1} \beta), \quad (16)$$

where

$$\beta = \frac{\sqrt{2}Z^2}{1 - Z^2} \cdot \frac{(m_1 - m_2)^2 \phi_1 \phi_2 \sqrt{\omega/\omega_1^c}}{g_1 + g_2 Z \sqrt{\omega_2^c/\omega_1^c}} \quad (17)$$

$$m_j = \frac{\alpha_j M_j}{E_{Gj}}, \quad g_j = \sqrt{\frac{(1 - \alpha_j m_j) m_j \gamma_j}{\alpha_j}}, \quad \omega_j^c = \frac{\phi_j \eta_j}{\kappa_j \rho_{fj}}, \quad \gamma_j = \frac{\phi_j \rho_{fj}}{\rho_j}, \quad (18)$$

$$Z = \sqrt{\frac{\rho_2 E_{G2}}{\rho_1 E_{G1}}}, \quad E_{Gj} = E_{mj} + \alpha_j^2 M_j, \quad E_{mj} = K_{mj} + 4\mu_j/3, \quad (19)$$

$$M_j^{-1} = (\alpha_j - \phi_j)/K_{sj} + \phi_j/K_{fj}, \quad \alpha_j = 1 - K_{mj}/K_{sj}, \quad (20)$$

$$\rho_j = (1 - \phi_j)\rho_{sj} + \phi_j\rho_{fj}, \quad (21)$$

where ω is the angular frequency, K_m and μ are the dry-rock bulk and shear moduli, respectively, ρ_s and ρ are the solid and bulk densities, respectively, κ is permeability, and $i = \sqrt{-1}$.

A.2 Gurevich et al. Equations

Gurevich et al. (2004) approximations of the wavenumbers of the fast and slow waves are (their Eqs. 10 and 11),

$$l_1 \approx \omega \sqrt{\frac{\rho}{E_G}}, \quad l_2 \approx \sqrt{\frac{i\omega\eta E_G}{\kappa M E_m}}, \quad (22)$$

to be compared with the exact ones, obtained from the dispersion Eq. (5).

Gurevich et al. (2004, Eq. 22) PP reflection coefficient is

$$R = \frac{1 - (1 - X)Z}{1 + (1 + X)Z}, \quad (23)$$

where

$$X = \frac{\sqrt{-i\omega\rho_1 E_{G1}} \cdot (m_1 - m_2)^2}{P_1 + P_2}, \quad (24)$$

$$P_j = \sqrt{\frac{\eta_j M_j E_{mj}}{\kappa_j E_{Gj}}}. \quad (25)$$

A.3 Silin and Goloshubin expression

The normal-incidence PP reflection coefficients at an interface separating the incidence medium 1 and the transmission medium 2 reported by Silin and Goloshubin (2010, their Eq. 88; see Eqs. 9, 15, 24, 35, 64, 75, 78, 84-87) is

$$R_k = r_0 + r_1 \sqrt{\epsilon_k}, \quad \epsilon = \frac{i\omega\kappa\rho_f}{\eta}, \quad (26)$$

where

$$r_0 = \frac{I_1 - I_2}{I_1 + I_2}, \quad r_1 = \frac{t - r}{I_1 + I_2} \cdot I_2, \tag{27}$$

$$I_j = \frac{E_{mj}}{v_{mj}} \sqrt{\frac{u_j}{\xi_j}} = \sqrt{\rho_j E_{mj}} \sqrt{\frac{u_j}{\xi_j}}, \quad u_j = \zeta_j^2 + \xi_j, \tag{28}$$

$$\xi_j = \left[\frac{\phi_j}{K_{fj}} + \frac{(K_{sj} - K_{mj})(1 - \phi_j)}{K_{sj}^2} \right] K_{mj}, \quad \zeta_j = 1 - \frac{K_{mj}(1 - \phi_j)^2}{K_{sj}}, \tag{29}$$

$$r = \frac{Au_2}{D\zeta_2}, \quad t = \frac{Au_1}{D\zeta_1}, \tag{30}$$

$$D = \frac{1}{\zeta_1 \zeta_2} \cdot \left(\frac{E_{m2} u_1 \sqrt{u_2}}{\sqrt{\bar{\epsilon}} v_{f2}} + \frac{E_{m1} u_2 \sqrt{u_1}}{v_{f1}} \right), \tag{31}$$

$$A = \frac{2I_1 I_2}{I_1 + I_2} \left(\frac{\zeta_1}{u_1} - \frac{\zeta_2}{u_2} \right), \tag{32}$$

$$v_{mj} = \sqrt{\frac{E_{mj}}{\rho_j}}, \quad v_{fj} = \sqrt{\frac{E_{mj}}{\rho_{fj}}}, \quad \bar{\epsilon} = \frac{\epsilon_2}{\epsilon_1}. \tag{33}$$

Note that I_j [Eq. (28)] are not Gassmann impedances ($\sqrt{\rho_j E_{mj}}$) as in the other approximations. Since subindex k is undetermined in Silin and Goloshubin (2010) [see Eq. (26)], we consider two reflections coefficients, corresponding to ϵ of medium 1 ($k = 1$) and ϵ of medium 2 ($k = 2$).

Funding Funding was provided by Jiangsu Province Science Fund for Distinguished Young Scholars (Grant Number BK20200021), the National Natural Science Foundation of China (grant no. 41974123) and the Jiangsu Innovation and Entrepreneurship Plan.

References

Allard JF (1993) Propagation of sound in porous media, modelling sound absorbing materials. Elsevier Sci. Pub. Ltd., London

Biot MA (1956a) Theory of propagation of elastic waves in a fluid-saturated porous solid. I. Low-frequency range. *J Acoust Soc Am* 28:168–178

Biot MA (1956b) Theory of propagation of elastic waves in a fluid-saturated porous solid. II. High-frequency range. *J Acoust Soc Am* 28:179–191

Biot MA (1962) Generalized theory of acoustic propagation in porous dissipative media. *J Acoust Soc Am* 34:1254–1264

Bourbie T, Coussy O, Zinzner B (1987) Acoustics of porous media. Gulf Publishing Company, Houston

- Carcione JM (1998) Viscoelastic effective rheologies for modeling wave propagation in porous media. *Geophys. Prosp.* 46:249–270
- Carcione JM (2014) *Wave fields in real media. Theory and numerical simulation of wave propagation in anisotropic, anelastic, porous and electromagnetic media*, 3rd edn, revised and extended, Elsevier Science
- Carcione JM, Campanella O, Santos JE (2007) A poroelastic model for wave propagation in partially frozen orange juice. *J Food Eng* 80:11–17
- Carcione JM, Picotti S (2006) P-wave seismic attenuation by slow-wave diffusion. Effects of inhomogeneous rock properties. *Geophysics* 71:O1–O8
- Carcione JM, Quiroga-Goode G (1995) Some aspects of the physics and numerical modeling of Biot compressional waves. *J Comput Acoust* 3:261–280
- Denneman AIM, Drijkoningen GG, Smeulders DMJ, Wapenaar K (2002) Reflection and transmission of waves at a fluid/porous-medium interface. *Geophysics* 67:282–291
- Deresiewicz H, Rice JT (1964) The effect of boundaries on wave propagation in a liquid-filled porous solid: V. Transmission across a plane interface. *Bull Seism Soc Am* 54:409–416
- Deresiewicz H, Skalak R (1963) On uniqueness in dynamic poroelasticity. *Bull Seism Soc Am* 53:783–788
- Dutta NC, Odé H (1983) Seismic reflections from a gas-water contact. *Geophysics* 48:1–2
- Geertsma J, Smit DC (1961) Some aspects of elastic waves propagation in fluid-saturated porous solids. *Geophysics* 26:169–181
- Goloshubin G, Silin D, Vingalov V, Takkand G, Latfullin M (2008) Reservoir permeability from seismic attribute analysis. *Lead Edge* 27:376–381
- Gurevich B (1994) Discussion on: “Wave Propagation in heterogeneous, porous media: a velocity-stress, finite difference method,” by N. Dai, A. Vafidis, and E. R. Kanasewich (March–April 1995). *Geophysics* 327–340
- Gurevich B, Ciz R, Denneman AIM (2004) Simple expressions for normal incidence reflection coefficients from an interface between fluid-saturated porous materials. *Geophysics* 69:1372–1377
- Gurevich B, Lopatnikov SL (1995) Velocity and attenuation of elastic waves in finely layered porous rocks. *Geophys J Int* 121:933–947
- Gurevich B, Marschall R, Shapiro SA (1994) Effect of fluid flow on seismic reflections from a thin layer in a porous medium. *J Seism Explor* 3:125–140
- Gurevich B, Schoenberg M (1999) Interface boundary conditions for Biot’s equations of poroelasticity. *J Acoust Soc Am* 105:2585–2589
- Johnson DL (1982) Elastodynamic of gels. *J Chem Phys* 77:1531–1539
- Johnson DL, Koplik J, Dashen R (1987) Theory of dynamic permeability and tortuosity in fluid-saturated porous media. *J Fluid Mech* 176:379–402
- Johnson DL, Plona T (1982) Acoustic slow waves and the consolidation transition. *J Acoust Soc Am* 72:556–565
- Krief M, Garat J, Stellingwerff J, Ventre J (1990) A petrophysical interpretation using the velocities of P and S waves (full waveform sonic). *Log Analyst* 31:355–369
- Li S, Rao Y (2020) Seismic low-frequency amplitude analysis for identifying gas reservoirs within thinly layered media. *J Geophys Eng* 17:175–188
- Mavko G, Mukerji T, Dvorkin J (2009) *The rock physics handbook*. Cambridge Univ. Press, Cambridge
- Pride SR, Harris JM, Johnson DL, Mateeva A, Nihel KT, Nowack RL, Rector JW, Spetzler H, Wu R, Yamamoto T (2003) Permeability dependence of seismic amplitudes. *Lead Edge* 22:518–525
- Quiroga-Goode G, Carcione JM (1997) Wave dynamics at an interface in porous media. *Boll Geos Teor Appl* 38:165–178
- Rasolofosaon PNJ (1988) Importance of interface hydraulic condition on the generation of second bulk compressional wave in porous media. *Appl Phys Lett* 52:780–782
- Rosenbaum JH (1974) Synthetic microseismograms: logging in porous formations. *Geophysics* 39:14–32
- Silin DB, Goloshubin GM (2010) An asymptotic model of seismic reflection from a permeable layer. *Transp Porous Media* 83:233–256
- Silin DB, Korneev VA, Goloshubin GM, Patzek TW (2006) Low-frequency asymptotic analysis of seismic reflection from a fluid-saturated medium. *Transp Porous Media* 62(3):283–305
- Xu D, Wang Y, Gan Q, Tang J (2011) Frequency-dependent seismic reflection coefficient for discriminating gas reservoirs. *J Geophys Eng* 8:508–513
- White JE, Mikhaylova NG, Lyakhovitskiy FM (1975) Low frequency seismic waves in fluid saturated layered rocks. *Izvestija Acad Sci USSR Phys Solid Earth* 11:654–659

Zhou D, Yin X, Zong Z (2020) Closed-form expressions of plane-wave reflection and transmission coefficients at a planar interface of porous media with a normal incident fast P-wave. *Geophys Pure Appl.* <https://doi.org/10.1007/s00024-019-02383-1>

Publisher's Note Springer Nature remains neutral with regard to jurisdictional claims in published maps and institutional affiliations.